Journal of
Applied Crystallography
ISSN 0021-8898

Received 16 August 2006
Accepted 23 January 2007

Homodyne and heterodyne X-ray photon correlation spectroscopy: latex particles and elastomers

F. Livet,[a]* F. Bley,[a] F. Ehrburger-Dolle,[b] I. Morfin,[b] E. Geissler[b] and M. Sutton[c]

[a]LTPCM-ENSEEG, UMR-CNRS 5614, INPG/UJF, BP 75, 38402 St Martin d'Hères, France, [b]LSP, UMR CNRS 5588 UJF, BP 87, 38402 St Martin d'Hères Cedex, France, and [c]Physics Department, McGill University, Montreal, Québec, Canada H3A 2T8. Correspondence e-mail: flivet@ltpcm.inpg.fr

In a coherent X-ray small-angle experiment, heterodyning between the scattering amplitudes of two samples is obtained by stacking a static reference and a fluctuating sample. Results of homodyne and heterodyne measurements are compared in the case of 98 nm diameter latex particles in glycerol. The method is also used for the study of the slow relaxation process of carbon-black-filled ethylene–propylene elastomers corresponding to the relaxation of the carbon black skeleton after a 100% elongation. On the scale of the 10 μm coherent beam, heterodyning is used to separate fluctuations from long-term flowing of the sample. We show that this flow can be observed for about 10 h, with velocities of the order of nanometres per second. Random fluctuations are dominant in the speckle changes only for large q values ($q > 2 \times 10^{-2}$ Å^{-1}) and after a long relaxation time.

1. Introduction

Since the pioneering work of Sutton *et al.* (1991), X-ray photon correlation spectroscopy (XPCS) has become a well established technique, and it provides a very good method for the study of fluctuations in soft condensed matter systems (*cf.* references [9]–[18] in Falus *et al.*, 2004). The main advantages of this method are that it opens up the possibility of measurements at large q values [$q = (4\pi/\lambda)\sin\theta > 0.01$ Å^{-1}, where λ is the X-ray wavelength and 2θ is the detection angle] and allows the study of systems which are optically opaque, like carbon-black-filled elastomers.

Another characteristic of coherent X-ray beams is in their small size. In an X-ray speckle experiment, a small part of the incoherent beam from a synchrotron is selected with a pinhole or with slits. The coherent beam size ϕ and the beam divergence ϵ must fulfil the (transverse) coherence conditions, which can be roughly written as

$$\phi \times \epsilon \leq \lambda. \quad (1)$$

For practical experiments, $\epsilon \simeq 10$ μrad, primarily because the CCD detectors used (Livet *et al.*, 2000) have a 20 μm resolution with a sample-to-detector distance of the order of 2 m. This means that $\phi \simeq 10$ μm, and that the irradiated surface is at least two orders of magnitude smaller than in light scattering (obviously, a laser beam can be focused to a size smaller than 10 μm, but its divergence due to diffraction gives an effective beam size of about 100 μm for a sample of a thickness in the millimetre range). This size ϕ can be further reduced with the new X-ray focusing elements (Schroer *et al.*, 2003; Di Fabrizio *et al.*, 1999).

In a small-angle X-ray scattering (SAXS) experiment, the longitudinal coherence condition, which states that interference along the beam path can occur if the path-length variation $\Delta\mathcal{L}$ is smaller than $\delta\lambda/(2\lambda^2)$, is often satisfied for small θ values, provided the sample thickness e satisfies

$$\Delta\mathcal{L} \simeq 2e \times \theta^2 < \Lambda_1 = \lambda^2/2\delta\lambda. \quad (2)$$

For small enough θ, with a sample thickness of the order of one millimetre, coherent SAXS experiments can be carried out with a 'pink beam' (Abernathy *et al.*, 1998) obtained by selecting a harmonic of the undulator with mirrors and filters ($\delta\lambda/\lambda \simeq 1\%$ r.m.s.).

In this paper, we report experiments with a Ge_{111}-monochromated beam [$\lambda^2/(2\delta\lambda) \simeq 0.25$ μm, $\lambda \simeq 1.6$ Å) obtained at the IMMY/XOR-CAT (8-ID) beamline at APS (Argonne, Illinois) (for a description, see Sandy *et al.*, 1999). In these experiments, flat (non-focusing) optics were used, the coherent beam was selected by means of 15×15 μm^2 square slits 0.64 m upstream of the sample, guard slits close to the sample were added, the beam intensity was in the 10^9 photons s^{-1} range, the sample-to-detector distance was 2.8 m and the detector resolution was 22.5 μm.

In equation (2), the sample thickness e for the θ range studied can be of the order of one centimetre, and this property is used for carrying out heterodyne measurements where interferences are obtained between the SAXS amplitude from a stable reference (an aerosil) and that of a fluctuating sample. These two samples have millimetre thicknesses, and they are simply stacked, with the aerosil upstream. By moving the hybrid sample in the beam, the scattering of the fluctuating sample alone ('homodyne') or that of both ('heterodyne') can be obtained allowing the results of the two methods to be compared.

Heterodyning was also used by Eisebitt *et al.* (2003) for soft X-rays by splitting the X-ray coherent beam transversally by means of a small aperture and by Gutt *et al.* (2003), where the reference signal was obtained through a fortuitous overlap of the specular and diffuse reflected scattering. More recently, heterodyning has been observed by interferences between fluctuating and non-fluctuating amplitudes in smectic membranes (de Jeu *et al.*, 2005).

In this paper, we show that by simply using a static random scatterer, heterodyning with X-rays can be performed in a controlled way

in a small-angle configuration. We demonstrate the technique by studying the Brownian motion of latex spheres in glycerol and also by performing velocity measurements in a model rubber system of ethylene–propylene elastomers filled with carbon black particles.

2. Homodyne and heterodyne correlations in a latex suspension

A suspension of spherical latex particles (98 nm diameter, concentration 10%, temperature 283 K) in glycerol has been used for testing the method. This system was studied by Lumma, Lurio, Borthwick *et al.* (2000) by homodyne methods. As the fluctuation times of this system are sub-second, the kinetic mode of the CCD was used (Lumma, Lurio, Mochrie & Sutton, 2000). In our experiment, the CCD was divided into 18 strips of 64 rows and the irradiated region was limited by means of slits. For each frame, the measured intensity was analysed with the 'droplet algorithm' (DA), which, for low counting rates, transforms the direct-illumination CCD in a photon-counting area detector (Livet *et al.*, 2000). The elementary kinetic shift times δt were 25, 150, 350 and 1000 ms. Fig. 1 shows a small part of the 1242 × 1152 CCD in a homodyne measurement. In this figure, the scattering of the latex suspension is shown after each frame has been transformed by the DA and 200 frames of 25 ms shift times have been added. The intensity scale is logarithmic, and one observes 0 (black) to 50 (violet) photons per pixel. Between two strips, a blind region is obtained by suitably closing the slits in front of the detector, and this ensures no overlap between these strips. The latex particle scattering is clearly oscillating, and the first minimum (close to the horizontal pixel 400) is in good agreement with the 98 nm diameter spherical particle form factor.

The incoherent intensities obtained by angular averaging of our measurements are plotted in Fig. 2 for the three measurements described in §1. For comparison, data have been normalized to counts per pixel per second for a 10^9 photons s^{-1} beam intensity with an absorption correction. This figure shows the observed scattering from the hybrid sample $\langle I_t(\mathbf{q})\rangle$, the intensity of the fluctuating sample corrected for the static aerosol transmission $\langle I_s(\mathbf{q})\rangle \times \mathrm{tr_a}$ ($\mathrm{tr_a} \simeq 0.086$) and the aerosol intensity corrected for the latex sample transmission $\langle I_a(\mathbf{q})\rangle \times \mathrm{tr_s}$ ($\mathrm{tr_s} \simeq 0.21$): $\langle I_t\rangle = \langle I_a\rangle \times \mathrm{tr_s} + \langle I_s\rangle \times \mathrm{tr_a}$. Here, the incoherent intensities are calculated by averaging over a set of pixels P having the same q value in each strip, over the number M (= 15) of equivalent strips and over the number of frames N (30 of 1 s). P is of the order of 10^3 and the set of q values has been defined as $q - \delta q/2 < |\mathbf{q}| < q + \delta q/2$, with increasing δq and a constant $\delta q/q$.

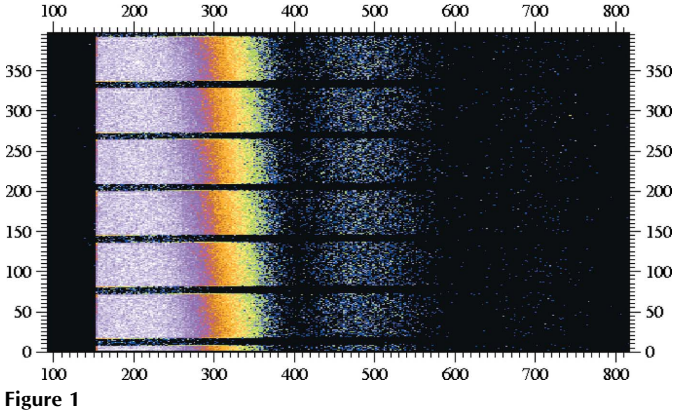

Figure 1
The result of adding 200 frames with 25 ms shift time when the CCD has been transformed to a photon-counting detector. This figure corresponds to a homodyne latex measurement. A total of 18 strips of period 64 rows are obtained (kinetic mode). The maximum intensity is 50 and individual counts are observed on this log scale. One pixel is 3.8×10^{-5} Å^{-1}.

From Fig. 2, the latex contribution to the scattering of the hybrid sample is less than 10%, and we define

$$x(q) = \langle \mathrm{tr_a} \times I_s(q)\rangle / \langle I_t(q)\rangle, \tag{3}$$

and from Fig. 2, $x(q)$ has a maximum value of about 0.08 for $q \simeq 6 \times 10^{-3}$ Å^{-1}. Time correlations are obtained from a comparison of the different strips in each frame. In practice, only 15 different equivalent strips are taken into account, which means that from a single series of measurements with a shift time δt, results are obtained only for times $\delta t, 2\delta t, \ldots, 14\delta t$. In the interpretation of these results, homodyne correlations are written

$$g^{(1)}(q,t) = \langle I_s(\mathbf{q}, t+t') I_s(\mathbf{q}, t)\rangle / \langle I_s(\mathbf{q}, t)\rangle^2. \tag{4}$$

$g^{(1)}$ can be written as

$$g^{(1)}(q,t) = 1 + \beta \exp[-t/\tau_1(q)]. \tag{5}$$

β is the coherence factor of the experiment which is constant for q values in this range and $\tau_1(q)$ is the correlation time. An estimate can be obtained from the angular speckle variations of the aerosol sample ($\beta \simeq 0.34$) or from the zero-time limit of $g^{(1)}(q,t)$. The exponential behaviour corresponds to the latex particle diffusion process measured by homodyne fluctuations.

Heterodyne correlations are defined here from

$$g^{(2)}(q,t) = \langle I_t(\mathbf{q}, t+t') I_t(\mathbf{q}, t)\rangle / \langle \langle I_t(\mathbf{q}, t)\rangle_t^2 \rangle_q. \tag{6}$$

In equation (6), the averages in the denominator have been split between time (the various frames) and q (the P pixels of a strip) so that $g^{(2)}$ can be written

$$g^{(2)}(q,t) = 1 + [2x(q)\beta/(1+\beta)] \exp[-t/\tau_1(q)]. \tag{7}$$

The Siegert relation states that the heterodyne $\tau_1(q)$ is twice the homodyne value.

In Fig. 3, the two functions $g^{(1)}(q,t)$ and $g^{(2)}(q,t)$ are plotted for the same q and for the same experimental conditions (same time series, same q). The zero-time intercept of $g^{(1)}$ yields $\beta \simeq 0.34$, and that of $g^{(2)}$ is $2x(q)\beta/(1+\beta) \simeq 0.03$, leading to a mixing of $x \simeq 0.06$, which agrees with Fig. 2. In Fig. 2, the correlation function does not decay to unity because only a fraction of the scattering (that of the sample) is fluctuating.

The statistical errors on these functions $g^{(1)}(q,t)$ and $g^{(2)}(q,t)$ have been estimated assuming low counting statistics:

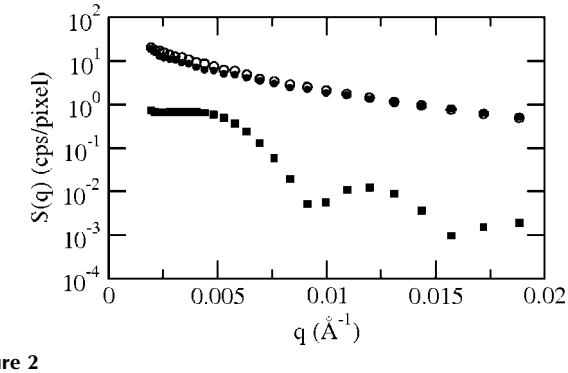

Figure 2
Isotropically averaged cross sections, normalized to compare the hybrid sample (aerosol + latex: open circles) count rate (in photons s^{-1} $pixel^{-1}$ for a 1×10^9 photons s^{-1} beam intensity) with the latex sample (closed squares) and the aerosol (closed circles).

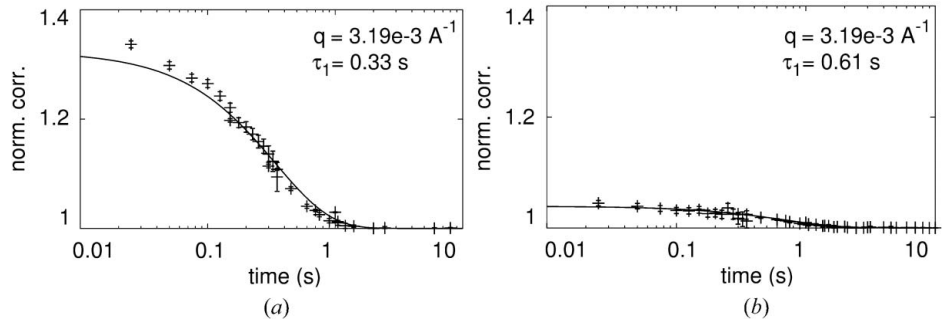

Figure 3
Correlations observed for $q = 3.19 \times 10^{-3}$ Å^{-1}. Left: homodyne; right: heterodyne. Continuous lines show the results of an exponential fit. The τ_1 values should differ by a factor two.

$$\Delta g(q, n\delta t) \simeq [g(q, n\delta t)]^{1/2}/\{I(q)\delta t[PN(M-n)]^{1/2}\}. \quad (8)$$

$I(q)$ is the hetero/homodyne incoherent intensity in photons s^{-1} pixel^{-1}, and for a given shift time δt, the error bars are increasing with time ($t = n\delta t$), as observed in Fig. 3.

Fits of the correlations with equations (4) and (6) have been done using *gnuplot*, assuming independent statistical errors on the $g(q, t)$ functions. The results are summarized in Fig. 4.

This system was studied in detail in Lumma, Lurio, Borthwick *et al.* (2000), and we limit the discussion to the comparison of the precision of the two methods. All the results given here correspond to two identical sets of measurements carried out by moving the latex sample and the hybrid sample alternately in the beam. In Fig. 4, for the largest q, the ratio x becomes so small that the short time fluctuations are difficult to observe. In the intermediate range, for $q < 5 \times 10^{-3}$ Å^{-1}, the error bars in heterodyne τ_1 deduced from the fit are close to twice those from the homodyne results. This means that the relative errors in obtaining the fluctuation time are of the same order, although the beam intensity on the latex sample is reduced a factor of 12 by the aerosol sample upstream. The complete error calculation is complex, but heterodyning can become useful for systems that are prone to radiation damage. As control of the relative scattering intensity is easily achieved by varying the thicknesses of the sample and of the reference, some optimization becomes possible.

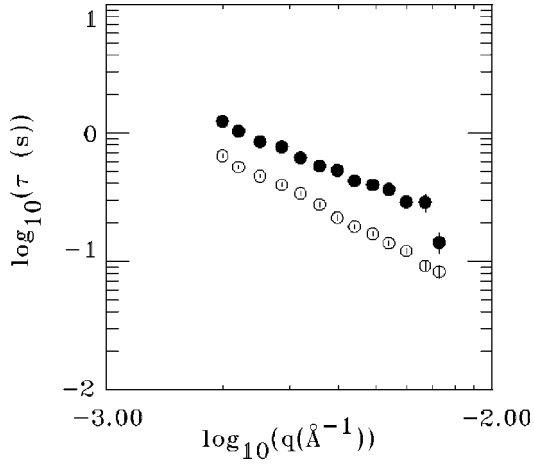

Figure 4
Correlation time τ_1 estimated for the latex particles from heterodyne and homodyne methods. The heterodyne times (closed circles) are always twice the homodyne ones (open circles) within the estimated errors.

3. Relaxation of filled polymers

Optically opaque carbon-black-filled polymers can be studied only by XPCS and heterodyning has been used for the study of the long-term relaxation of stretched samples. In a previous experiment carried out at the D2AM beamline (ESRF), we observed that the X-ray speckle fluctuations could be explained by a long-term drift (flowing) of the samples. These were 10% elongated and then the deformation was kept constant in order to study '*in situ*' the stress relaxation. We observed strong differences between cross-linked and uncross-linked ethylene–propylene rubbers (both with a 20% carbon black volume fraction).

One important problem in these rubber systems is to distinguish between random fluctuations and long-term flowing of the sample, which is always stressed when positioned in the beam. In Berne & Pecora (2000), a method based on heterodyning is proposed where the phase shift due to the relative velocity between the static reference and the moving sample is observed. This method was used for the study of the previous systems. Heterodyne and homodyne fluctuations were observed on samples which had been 100% elongated. The strain was then released, and the sample evolution was followed for some hours.

In this experiment, the heterodyne correlations $g^{(2)}$ were calculated in a different way from equation (6):

$$g^{(2)}(q, t) = \langle I_t(\mathbf{q}, t + t')I_t(\mathbf{q}, t)\rangle / \langle I_t(\mathbf{q}, t)\rangle^2. \quad (9)$$

In this case, $g^{(2)}(t = 0) = 1 + \beta$ and $g^{(2)}(t = \infty) > 1$, and such a calculation is necessary because the system is not ergodic, so that time averages (*i.e.* $t = \infty$ values) are not easy to estimate.

One can show that this new function $g^{(2)}$ can be written

$$g^{(2)}(q, \phi, t) = 1 + \beta(1-x)^2 + x^2\beta\gamma^2(t/\tau) + 2x(1-x)\beta\cos(\omega t)\gamma(t/\tau), \quad (10)$$

where ωt corresponds to the phase shift between the two amplitudes introduced by the relative movement $\mathbf{v}$ of the sample *versus* the aerosol, and $\omega = qv\cos\phi$, where ϕ is the angle between $\mathbf{v}$ and $\mathbf{q}$.

Fig. 5 shows some of the results obtained with the heterodyne correlation function $g^{(2)}$ for the cross-linked sample. In this figure are plotted the results of the fits with equation (10), assuming that the damping term $\gamma(t/\tau)$ in equation (10) had a compressed exponential behaviour $\{\gamma(t/\tau) = \exp[-(t/\tau)^{\mu})]\}$, as often observed in this type of 'jammed' system (Cipelletti *et al.*, 2003; Bandyopadhyay *et al.*, 2004). The four top figures examine for the same $|\mathbf{q}|$ value the angular dependence of $g^{(2)}$. We obtain a very precise estimate of ω from these results, and its linear dependence on $\cos(\phi)$ is well verified. In the four

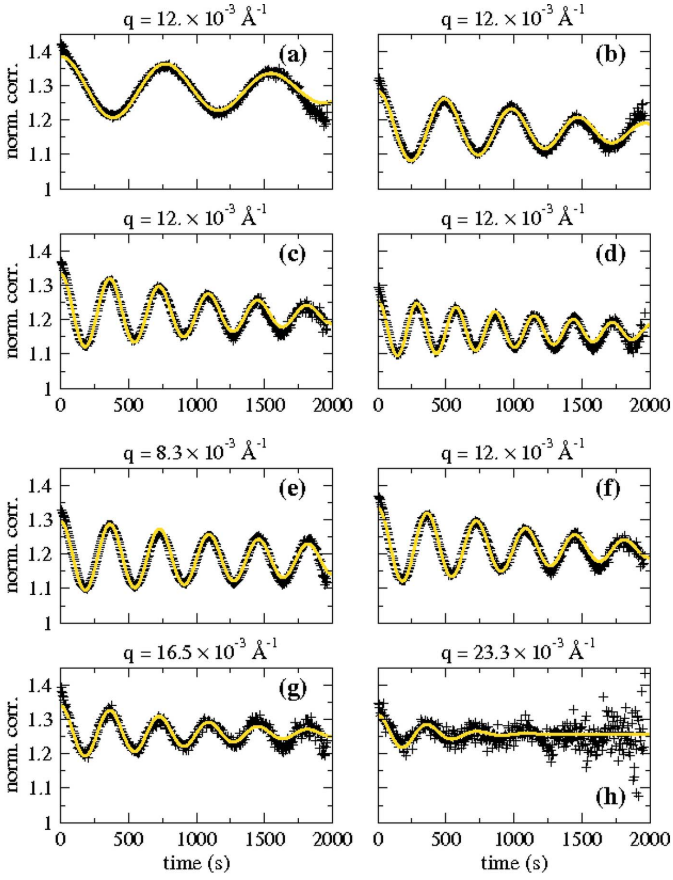

Figure 5
Oscillating behaviour of the normalized correlations for various q values and angles observed during relaxation of the cross-linked sample 20000 s after a 100% elongation: (a)–(d): same $|q| = 12 \times 10^{-3}$ Å^{-1}, but $q\cos(\phi) = 0.569$, 0.899, 1.21 and 1.52×10^{-3} Å^{-1}; (e)–(h): same $q\cos(\phi) = 1.21 \times 10^{-3}$ Å^{-1}, but various $|q|$ values.

lower curves, as $q\cos(\phi)$ is constant, the oscillations have the same period. By comparing these results, one can also observe the damping corresponding to random fluctuations in our sample. In the four top curves, the amplitude of the oscillations decrease by a factor of less than two in 2000 s and the estimate of a fluctuation time τ is imprecise. In the four lower curves, the damping becomes strong for large q values, but results are also very noisy. These curves use only a very small part of the detector, and fits with all data have to be done. The time evolution of the estimated velocity of the irradiated sample is plotted in Fig. 6, and we observe that the flowing of the sample is a very long process. Our method is able to measure velocities in the nm s^{-1} range.

4. Conclusion

The application of heterodyning to the relaxation of filled rubbers seems very promising. In the case studied here, this long-term relaxation corresponds to the reconstruction of the carbon black network after a large deformation, and new experiments have to be carried out with well controlled stress and strain. The first results described here nevertheless show that a careful analysis of a speckle experiment is necessary. When this was done, the fluctuations in the speckle structure are essentially explained by long-term sample movements. In the experiment described here, for $q < 1 \times 10^{-2}$ Å^{-1}, *i.e.* in the q domain of light scattering, no damping term is observed, and the decay in the correlation can be explained simply by the time it

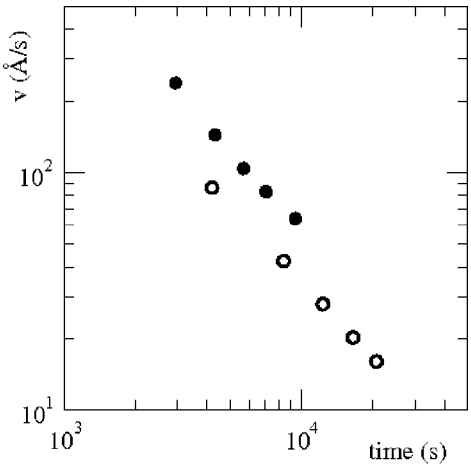

Figure 6
Relaxation of the velocities in both samples. The cross-linked specimen (open circles) is slower than the uncross-linked specimen (closed circles).

takes for the sample to flow out of the beam. The random fluctuations can be explained by a sample drift observed during 4 h after the sample has been placed in the beam. The random fluctuations are observed for larger q values from the damping $\gamma(t/\tau)$ term. We have checked that this term is independent of the angle ϕ, but its estimate from the restricted part of the experimental data which has been used is quite imprecise.

This may indicate that the small size of the X-ray coherent beam (10 µm) gives access to a different scale in these systems, the scattering of which in visible light would be interpreted by the 'jamming' model (Cipelletti *et al.*, 2003; Bandyopadhyay *et al.*, 2004), and in an X-ray experiment as a local flow of the sample. Further experiments are necessary for a better discussion, and X-ray heterodyning brings a new tool for the study of this problem.

Heterodyning between the amplitude scattered by two samples is a well established method. For radiation-sensitive materials the upstream absorption of the reference lowers irradiation and heterodyning also seems to give a better signal-to-noise ratio, but more work needs to be done to quantify this. The ability to observe the velocity demonstrates that the phase can be directly measured and this opens up many new possibilities of the technique. Finally, we have the ability to separate advection terms (like flow) from the dissipative terms (like diffusion) in the equation of motion of the system.

Use of the Advanced Photon Source was supported by the US Department of Energy, Office of Science, Office of Basic Energy Sciences, under Contract No. W-31-109-Eng-38.

References

Abernathy, D. L., Grübel, G., Brauer, S., McNulty, I., Stephenson, G. B., Mochrie, S. G. J., Sandy, A. R., Mulders, N. & Sutton, M. (1998). *J. Synchrotron Rad.* **5**, 37–47.
Bandyopadhyay, R., Liang, D., Yardimci, H., Sessoms, D. A., Borthwick, M. A., Mochrie, S. G. J., Harden, J. L. & Leheni, R. L. (2004). *Phys. Rev. Lett.* **93**, 228302.
Berne, B. J. & Pecora, R. (2000). *Dynamic Light Scattering*. New York: Dover Publications.
Cipelletti, L., Ramos, L., Manley, S., Pitard, E., Weitz, D. A., Pashkovski, E. E. & Johansson, M. (2003). *Faraday Discuss.* **123**, 237–251.
Di Fabrizio, E., Romanato, F., Gentil, M., Cabrini, S., Kaulich, B., Susini, J. & Barett, R. (1999). *Nature (London)*, **401**, 895–898.

Eisebitt, S., Lörgen, M., Eberhardt, W., Lüning, J., Stöhr, J., Rettner, C. T., Hellwig, O., Fullerton, E. E. & Denbeaux, G. (2003). *Phys. Rev. B*, **68**, 104419.

Falus, P., Borthwick, M. A. & Mochrie, S. G. J. (2004). *Rev. Sci. Instrum.* **75**, 4383–4400.

Gutt, C., Ghaderi, T., Madsen, A., Seydel, T., Tolan, M., Sprung, M., Grübel, G. & Sinha, S. K. (2003). *Phys. Rev. Lett.* **91**, 076104.

Jeu, W. H. de, Madsen, A., Sikharulidze, I. & Sprunt, S. (2005). *Physica B*, **357**, 39–44.

Livet, F., Bley, F., Mainville, J., Sutton, M., Mochrie, S. G. J., Geissler, E., Dolino, G., Abernathy, D. L. & Grübel, G. (2000). *Nucl. Instrum. Methods A*, **451**, 596–609.

Lumma, D., Lurio, L. B., Borthwick, M. A., Falus, P. & Mochrie, S. G. J. (2000). *Phys. Rev. E*, **62**, 8258–8269.

Lumma, D., Lurio, L. B., Mochrie, S. G. J. & Sutton, M. (2000). *Rev. Sci. Instrum.* **71**, 3274–3284.

Sandy, A. R., Lurio, L. B., Mochrie, S. G. J., Malik, A., Stephenson, G. B., Pelletier, J. F. & Sutton, M. (1999). *J. Synchrotron Rad.* **6**, 1174–1184.

Schroer, C. G., Kuhlmann, M., Hunger, U. T., Günzler, T. F., Kurapova, O., Feste, S., Frehse, F., Lengeler, B., Drakopoulos, M., Somogyi, A., Simionovici, A. S., Snigirev, A., Snigireva, I., Schug, C. & Schröder, W. H. (2003). *Appl. Phys. Lett.* **82**, 1485–1487.

Sutton, M., Mochrie, S. G. J., Greytak, T., Nagler, S. E., Berman, L. E., Held, G. E. & Stephenson, G. B. (1991). *Nature (London)*, **352**, 608–610.